Computed Tomography in 75 Clinical Cases of Syringomyelia

M. L. Aubin[1]
J. Vignaud
C. Jardin
D. Bar

Seventy-five patients with a clinical diagnosis of syringomyelia were examined by computed tomography after intrathecal injection of metrizamide. A central cavity was demonstrated in 67 patients. Tilting the patient head down did not increase the rate of cavity opacification. This evidence favors transneural migration of metrizamide into the cavity. The spinal cord was measurably enlarged in only a minority of the patients. In some, the cavity appeared to have clefts or wall defects. These results are discussed according to the etiopathogenic theories advanced by Gardner, Aboulker, and Williams.

The anatomic basis for the clinical syndrome of syringomyelia is a cavity inside the spinal cord. This cavity may be a dilated central canal (hydromyelia), a cyst within the parenchyma (syringomyelia), or both (syringohydromyelia). Several theories have been proposed to explain the phenomenon of syringomyelia. According to Gardner et al. [1–3] (fig. 1A) failure of the foramina of the fourth ventricle to open at the 29th week of fetal life with continuing communication between the fourth ventricle and the central canal allows increased pressure within the ventricles to be transmitted to the central canal, which dilates. At the same time, the hydrocephalus causes inferior displacement of the cerebellum, thus creating an Arnold-Chiari malformation.

In the Williams [4] theory (fig. 1B), the resulting anatomic abnormality is approximately the same, except for the often observed lack of hydrocephalus. According to this theory, efforts such as the Valsalva maneuver produce increased venous pressure, which raises the cerebrospinal fluid pressure within the ventricles, which in turn is transmitted to the central canal, whereas muscular efforts induce venous hypertension in the medullary veins and in the cavity.

Aboulker [5] believes that the Gardner et al. [1–3] theory is only valid for children who have hydrocephalus frequently associated with meningocele. According to Aboulker (fig. 1C), the pathogenesis of the clinical syndrome of the syringomyelia in adults is different: a cavity develops within the parenchyma without any relation to the central canal which, in adults (according to pathologists mentioned by Aboulker [6–8]) is often collapsed, closed, or absent. The abnormality is caused by stenosis at the level of the foramen magnum due to Arnold-Chiari malformation, arachnoiditis, or tumors.

This theory is supported by canine experiments performed by Sato et al. [9] that demonstrated that 30% of cerebrospinal fluid is produced in the spinal canal. Due to the stenosis at the foramen magnum, the cerebrospinal fluid finds its way with difficulty towards the intracranial areas of resorption. The pressure of the cerebrospinal fluid within the spinal canal is higher than that of intracranial cerebrospinal fluid, resulting in edema within the cord. The last phase of this edema is a cavity. This mechanism is potentiated by increased venous pressure in the azygos system, which may be congenital or acquired.

According to Aboulker [5], the cerebrospinal fluid filters through the parenchyma or via a pathway along the posterior roots. Ball and Dayan [10] thought

Received June 11, 1980; accepted after revision October 16, 1980.

[1]All authors: Department of Radiology, Fondation A. de Rothschild, 29 Rue Manin, Paris XIX, France. Address reprint requests to M. L. Aubin.

AJNR 2:199–204, May/June 1981
0195–6108/81/0203–0199 $00.00

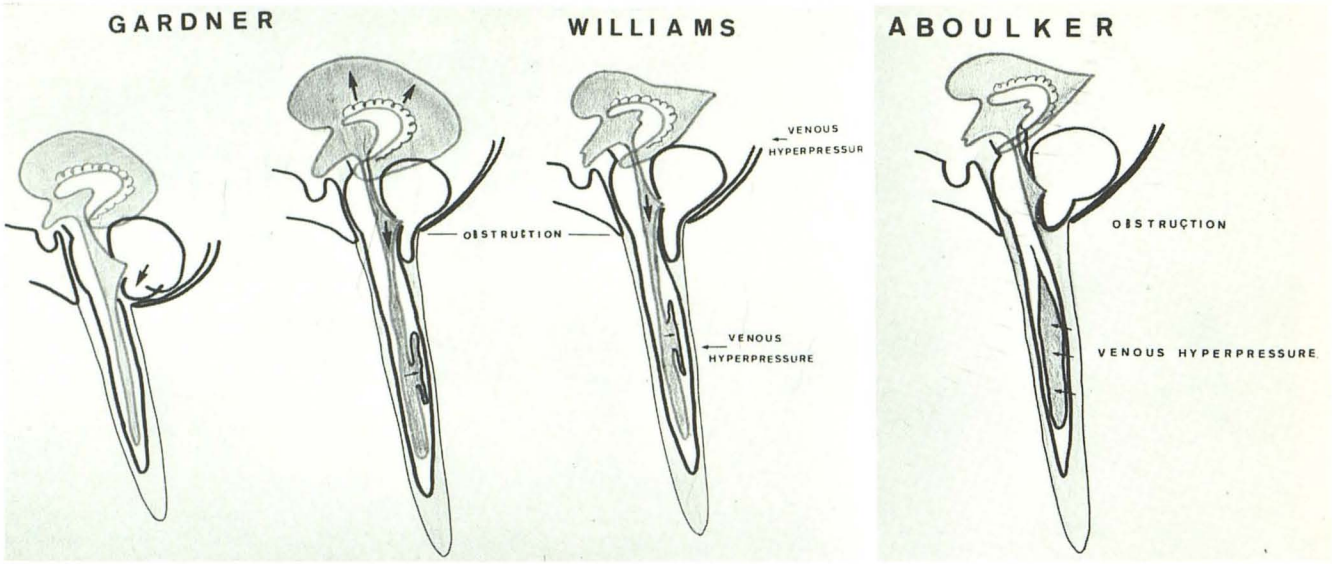

Fig. 1.—*Gardner theory* [1–3]. Failure of fourth ventricular foramina to open results in persistent communication between fourth ventricle and central canal. Resulting hydrocephalus causes increased pressure within central canal and inferior displacement of tonsils. *Williams theory* [4]. Intermittent venous hypertension results in increased cerebrospinal fluid pressure, which is transmitted to persistent central canal. *Aboulker theory* [5]. Incomplete cistern obstruction-hydrocephalus. High venous pressure with transmedullary passage of cerebrospinal fluid creating true syringomyelia cavity.

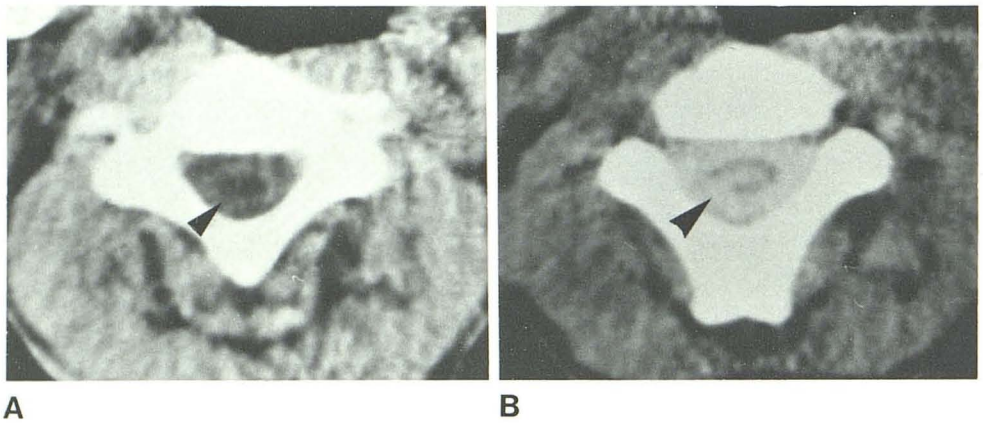

Fig. 2.—Comparison of visibility of syringomyelic cavity. **A**, Plain examination. **B**, Cavity opacification 6 hr after injection. On **B**, posterolateral defect of cyst is seen (*arrowhead*).

that it might be transmitted along the arteries. The cavity, which generally ends at the level of C2, may sometimes dissect along the medulla oblongata to reach the fourth ventricle. To obtain further information on the hydrodynamics of syringomyelia, we studied a large group of patients with metrizamide, observing its distribution in the spinal fluid and the syrinx cavity itself with computed tomography (CT).

Subjects and Methods

Seventy-five patients with clinically identified syringomyelia were referred to us for examination by CT. The patients were 12–70 years old (average, 40 years). There were no young children. Symptoms had been present for 3 months to 45 years (mean, 7 years). Only one patient had a history of remote trauma; none had a tumor.

All patients were scanned at least three times. Scans were obtained before (scan 0) and after metrizamide (7 ml of 170 mg I/ml) injected via lumbar approach. Scan 1 was obtained 10–30 min after injection. Then, at least one delayed scan (scan 2) was obtained at about 6 hr. Some of the patients were scanned 12, 24, or even 48 hr later. The scans were obtained with an Acta Pfizer 200 FS. The sections were usually 5 mm thick, sometimes 8 mm. Adjacent sections were scanned to allow sagittal and coronal reconstruction when necessary.

One group of patients (64 cases) was tilted head down, 1 min prone and 1 min supine. Another group (11 cases) was not tilted to try to maintain normal physiologic relations.

In the group that was tilted, the cervical spine and posterior fossa were studied. Two sections were scanned to check the lateral ventricles and the cerebral hemispheres. In the group that was not tilted, in addition to the above areas, the lumbar and thoracic spines were scanned every 2 cm.

In the last 21 tilted patients, serial density measurements of the subarachnoid space, cord, and cavity were made of one diameter of the spinal canal at about the same level in each patient. The

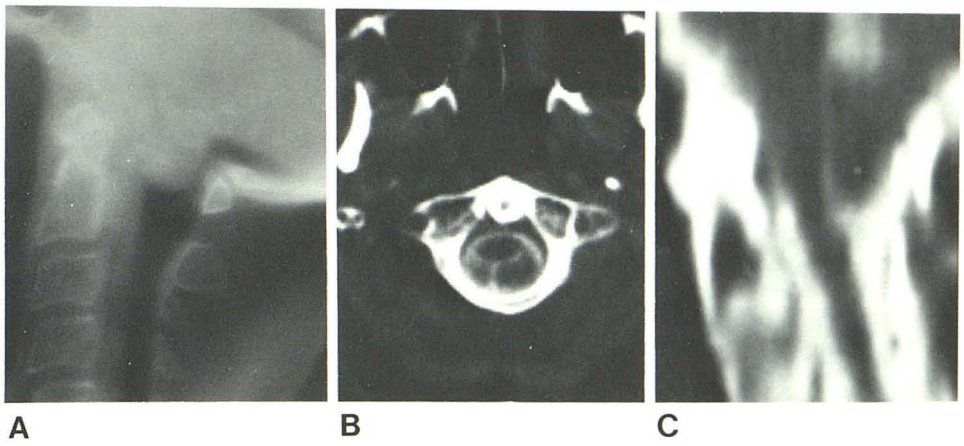

Fig. 3.—(Same patient as in fig. 2). Morphologic aspects of Arnold-Chiari I malformation with gas examination (**A**) and axial slice (**B**), and sagittal reconstruction (**C**) after metrizamide. Axial slice through CI shows tonsils behind cord in low position. Sagittal reconstruction demonstrates low position of fourth ventricle and tonsils.

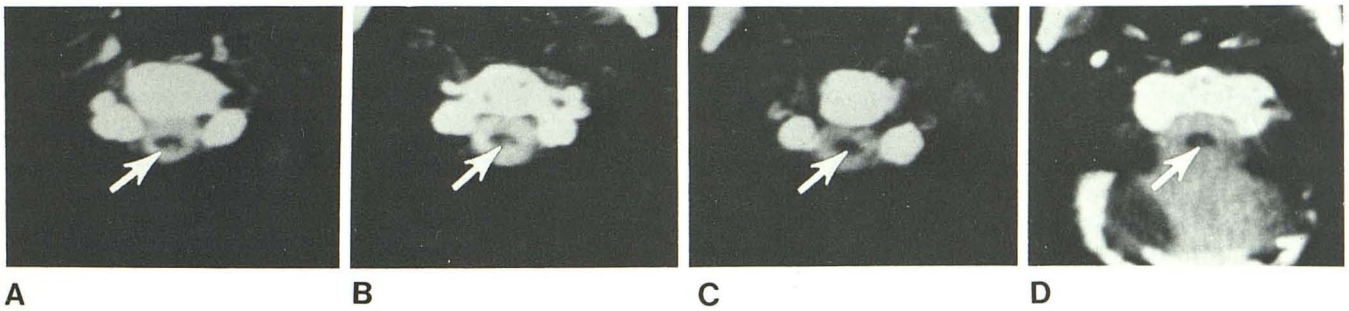

Fig. 4.—Four slices immediately after metrizamide injection. Central medullary hyperdensity (*arrows*) corresponds with persistent ependymal canal (Williams theory [4]).

Fig. 5.—Opacification of syringomyelic cyst 8 hr after injection. Posterolateral defect (*arrowhead*).

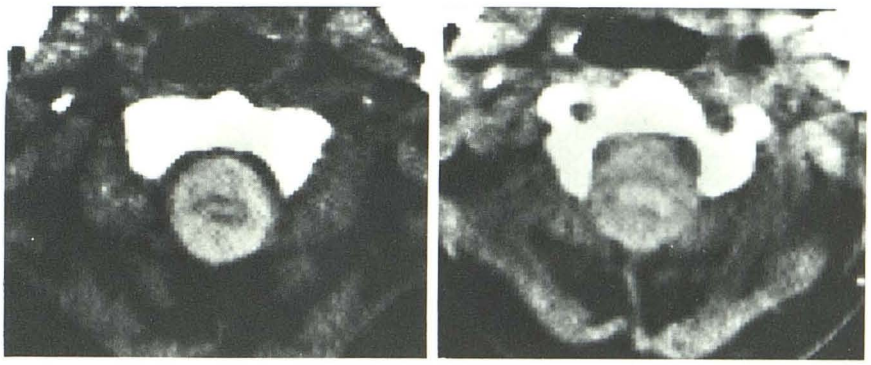

Fig. 6.—**A**, 14 hr after injection. Opacification of syringomyelic cyst. Patient had been operated on for Arnold-Chiari malformation. **B**, 20 hr after injection at same level. Metrizamide concentration in cyst and relative concentration decrease in subarachnoid spaces. Cord not really discernible from subarachnoid spaces.

diameters of the subarachnoid space, cord, cavity, and parenchyma were also measured. Ratios were obtained between diameters of cord and subarachnoid space.

Results

Tilted Patients

Scan 0. Among our 75 patients with clinical symptoms of syringomyelia, 67 had cavities demonstrated within the cord without metrizamide (fig. 2). The top level of the cavity was C2. The lateral ventricles were dilated in 17 cases. In nine of these (all older patients) there were also dilated sulci suggestive of atrophy. In eight cases there was true hydrocephalus, and among these the fourth ventricle was significantly dilatated in four. The ventricles were normal in the other cases.

Scan 1. Initial scans were obtained 10–30 min after injection of metrizamide. In all except one case the cisterns

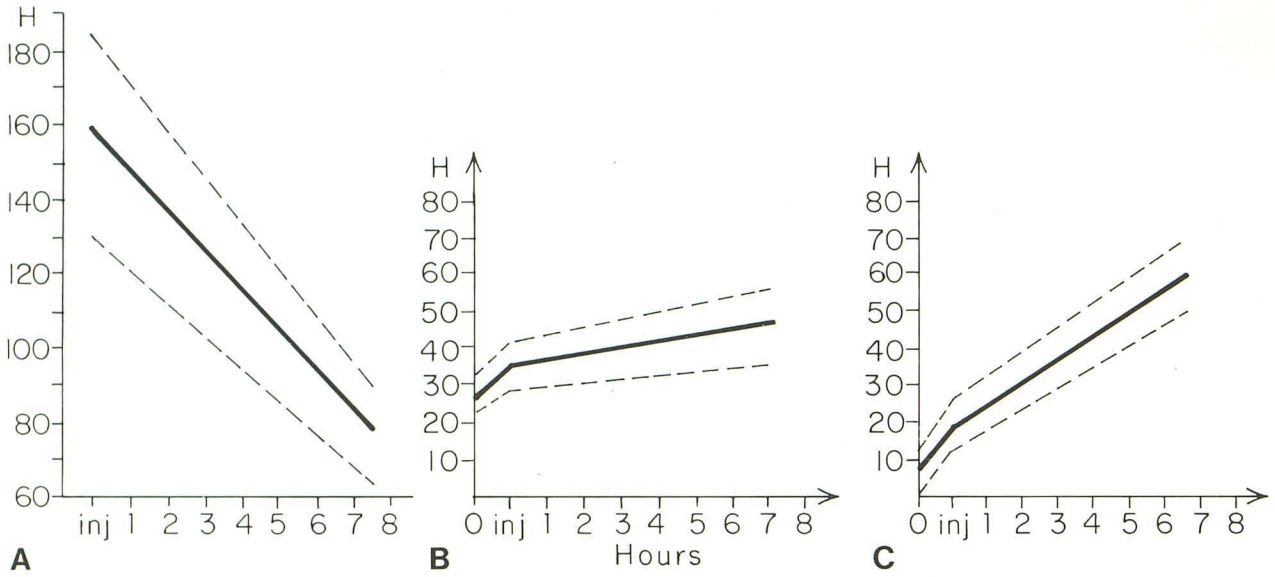

Fig. 7.—Relations between densities (in Hounsfield units) of subarachnoid space (**A**), cord (**B**), and cyst (**C**) and time of examination (in hours). Solid line = mean; dashed line = 1 SD.

of the posterior fossa and the base of the skull were opacified. Contrast material entered the fourth ventricle in 55 (86%) of the 64 tilted cases but did not in nine (14%) cases.

Arnold-Chiari malformation [19, 20] was demonstrated in 48 (79%) cases. Forty-seven were type I (fig. 3); one was a type II.

In all 64 cases, the opacified subarachnoid space sharply delineated the cord. The anteroposterior diameter of the subarachnoid space and cord were measured and the ratio of these diameters was calculated. According to the criteria of normal cord measurements established by Nordquist [11] at the C3–C4 level, we found three groups of measurements in 64 patients: enlarged cord (six cases); small cord (29 cases); and normal cord (29 cases).

Opacification of the cavity in the first 30 min occurred in only five of 64 cases (fig. 4). In the other 59 cases a cavity could not be clearly identified due to the high concentration of metrizamide, which necessitated wide window widths to visualize the cord. However, a density profile obtained on some of these cases demonstrated low density variations suggesting a cyst.

Scan 2. The second scan was obtained 6 hr after injection (±2 hr). A central cavity was opacified in 59 of 64 cases. Fifty-one of the cavities were first demonstrated without metrizamide; after metrizamide eight more were seen in small cords. In these cases, the cord parenchyma is thin. In nine of 59 cases, a posterolateral defect of the parenchyma was clearly visualized, on one (two cases) or both (seven cases) sides (figs. 2B–5). In four patients with hydrocephalus, the central cavity seen in the scan before metrizamide was not filled by metrizamide.

Delayed scans were obtained in six cases at 12, 24, and (in one case) 48 hr. The cavity usually remained opacified whereas the density of cerebrospinal fluid and parenchyma decreased.

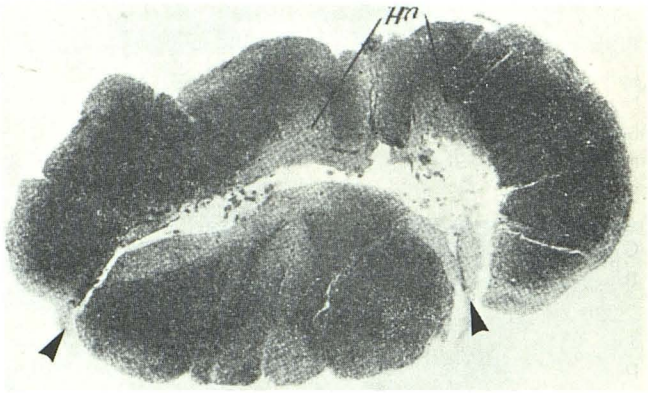

Fig. 8.—Cord anatomic slice in syringomyelic case. Posterior defects correspond to syringomyelic cavity (*arrowheads*). (Reprinted from [24].)

Density measurements. Evolution of the densities of the cerebrospinal fluid, cord, and cavity with time is demonstrated in figure 6. In 21 cases with density measurements, the mean densities of the cerebrospinal fluid and cord parenchyma were plotted against time (fig. 7). The curves demonstrate that in all these cases, there is an increase in density of the parenchyma and a much greater increase in density of the cystic cavity. On the other hand, cerebrospinal fluid density decreased with time, suggesting an active filling of the cavity with metrizamide. Delayed scans confirmed these findings. The density of the cavity remains high, whereas the density of the parenchyma and the cerebrospinal fluid decreased.

Nontilted Patients

Among the 11 nontilted patients, two had large laminectomies. In six cases syringomyelia was suspected on the

basis of gas myelography, and in three cases Arnold-Chiari malformation was diagnosed on the basis of myelobulbography.

CT was performed at the lumbar, thoracic, cervical, and cranial levels before and at 6, 12, and 24 hr after metrizamide injection. Even without tilting, eight of the 11 cysts were visible after the same delay as in tilted patients (6–12 hr).

Absorption coefficient measurements were obtained of the cord, the cyst, and the canal. However, the lack of tilting resulted in such metrizamide dilution that accurate density measurements were impossible. In one case, the examination failed to demonstrate a cyst because of metrizamide dilution. However, the premetrizamide scan showed a remarkably thin dorsal and cervical cord in this patient. In none of the 11 cases was there evidence that metrizamide had entered the fourth ventricle. The lateral ventricles were normal in all of the cases.

Discussion

Before CT, it was difficult to demonstrate the syringomyelic cavity consistently. In hydrocephalic children, ventriculography occasionally opacifies the cavity, thus demonstrating a communication between the fourth ventricle and the central canal, supporting the Gardner [1] theory. During myelography, accidental puncture of the cyst may occur [12], thus diagnosing syringomyelia. During gas myelography, a swollen cord is seen, which collapses after removal of cerebrospinal fluid and injection of contrast material.

CT is a better technique for visualization of the cavity. One may surmise that with the new generation of scanners, the accuracy will be even greater. The recognition of the cavity is somewhat more accurate with metrizamide [13–17]. Among 59 cavities visualized by metrizamide in tilted patients, eight were not visualized on the premetrizamide scans. In those instances, the cord was small.

In addition, the diagnosis of an Arnold-Chiari malformation is straightforward and accurate with CT [18–20]. In 48 of 59 cases who had an Arnold-Chiari malformation demonstrated by previous myelography, it was demonstrated as well by the metrizamide CT study. The ventricular system may be easily evaluated by CT and hydrocephalus demonstrated when present.

Concerning the pathogenesis of syringomyelia it should be noted that our series does not include young children. It represents only part of the population with clinical symptoms of syringomyelia.

In order to determine the possible route of metrizamide penetration, particular attention was paid to the 59 patients who had a cavity opacified. In only five cases was the central canal demonstrated on scan 1. This early filling of the cavity suggests that it fills from the region of the cisterna magna or fourth ventricle through the obex of a patent central canal. In these cases, the fourth ventricle and the cisterna magna were opacified after tilting.

In 54 cases, the filling was delayed. We cannot assess the exact time of the beginning of the filling because we did not obtain scans at frequent intervals and because of the possible error in the evaluation of the density measurements on the density profiles. But evidence of active filling of the cavity is convincing. It may be seen with a fourth ventricle filled or not. In cases of nontilted patients, the cavity was seen filled before the filling of intracranial cavities.

These observations and the time density curve strongly suggest transneural passage of metrizamide, which tends to support the Aboulker [5] theory. An analogy to normal pressure hydrocephalus can be made where metrizamide transport takes place through the brain parenchyma [21].

We know that metrizamide normally penetrates the brain parenchyma after intrathecal injection [22]. Dubois et al. [23] recently demonstrated this phenomenon in the dog's cord. However, because the cisterna magna was filled in all but one of our cases and because in most cases the fourth ventricle was filled also, we cannot eliminate the possibility of a microscopic passage of metrizamide through the obex and a narrow central canal not visible by CT because of poor spatial and density resolution. Thus, the metrizamide could leak into the cavity from above.

As to the "defects" observed in the parenchyma, it is tempting to identify them with parenchymal defects described by the pathologists, but the resolution of our scanner is insufficient (1 mm) to eliminate the possibility of a very thin wall of a parenchyma that could not be visualized (fig. 8).

Conclusions

Computed tomography in conjunction with intrathecal injection of metrizamide is an excellent method for the recognition of syringomyelia. It showed the syringomyelic cavity in 67 of 75 clinical cases. It is also good for the demonstration of the variable morphology of this condition. But, it has not been decisive in elucidating the pathogenesis of the process.

ACKNOWLEDGMENTS

We thank Larissa Bilaniuk and Patrick Turski for help in translation.

REFERENCES

1. Gardner W. Hydrodynamic mechanism of syringomyelia: its relationship to myelocele. *J Neurol Neurosurg Psychiatry* **1965**;28:247–259
2. Gardner W, Angel J. The mechanism of syringomyelia at its surgical correction. *Clin Neurosurg* **1975**;6:131–140
3. Gardner W, Murry FML. Noncommunicating syringomyelia: a nonexistent entity. *Surg Neurol* **1976**;6:251–256
4. Williams B. Pathogenesis of syringomyelia. *Lancet* **1972**;1:142–143
5. Aboulker J. La syringomyelie et les liquides intra rachidiens. *Neurochirurgie* **1979**;25:suppl 1
6. Greenfield J. *Neuropathology*. Arnold, **1976**
7. Escourolle R, Poirier J. Manuel élémentaires de neuropathologie. Paris: Masson, **1977**

8. Lichtenstein BW. *Syringomyelia—textbook of neuropathology*. London: Saunders, **1949**
9. Sato O, Asai T, Amono Y, Hara M, Tsugane R, Yagi M. Extraventricular origin of the cerebrospinal fluid: formation rate quantitatively measured in the spinal subarachnoid space of dogs. *J Neurosurg* **1972**;36:276–281
10. Ball MJ, Dayan AD. Pathogenesis of syringomyelia. *Lancet* **1972**;2:799–801
11. Nordquist L. The sagittal diameter of the spinal cord and subarachnoid space in different age groups. A roentgenographic postmorten study. *Acta Radiol* (Stockh) **1964**; Suppl 227
12. Ellertson AB. Syringomyelia and other cystic spinal cord lesions. *Acta Neurol Scand* **1969**;45:403–417
13. Vignaud J, Aubin ML. Computed tomography in 25 cases of syringomyelia. Presented at the annual meeting of the American Society of Neuroradiology, Toronto, Canada, April **1979**
14. Aubin ML, Vignaud J, Bar D, Jardin C. Apport de la scannographie à l'étude des syringomyelies. *Rev Neurol* (Paris) **1980**;136:271–277
15. Forbes W, Isherwood I. Computed tomography in syringomyelia and the associated Arnold Chiari I malformation. *Neuroradiology* **1978**;15:73–78
16. Bonafe A, Ethier R, Melancon D, Belanger G, Peters T. High resolution computed tomography in cervical syringomyelia. *J Comput Assist Tomogr* **1980**;4:42–47
17. Resjoe IM, Harwood-Nash DC, Fitz CR, Huang S. Computed tomographic metrizamide myelography in syringohydromyelia. *Radiology* **1979**;131:405–407
18. Naidich TP, Pudlowski RM, Naidich JB. Computed tomography signs of the Chiari II malformation. Part I—Skull and dural partitions. *Radiology* **1980**;134:65–71
19. Naidich TP, Pudlowski RM, Naidich JB. Computed tomography signs of the Chiari II malformation. Part II—Midbrain and cerebellum. *Radiology* **1980**;134:391–398
20. Naidich TP, Pudlowski RM, Naidich JB. Computed tomography signs of the Chiari II malformation. Part III—Ventricles and cisterns. *Radiology* **1980**;134:657–665
21. Hiratsuka H, Fujinara K, Okada K, Takasato Y, Tsumumu M, Inaba Y. Modification of periventricular hypodensity in hydrocephalus with ventricular reflux in metrizamide CT cisternography. *J Comput Assist Tomogr* **1979**;3 : 204–208
22. Winkler SS, Sackett JF. Explanation of metrizamide brain penetration: a review. *J Comput Assist Tomogr* **1980**;4:191–193
23. Dubois PJ, Drayer BP, Osborne D, Heintz ER. Intramedullary penetrance of metrizamide in the dog spinal cord. Presented at the annual meeting of the American Society of Neuroradiology, Toronto, Canada, May **1979**
24. Taylor J, Greenfield JC, Martin JP. Two cases of syringomyelia and syringobulbia. *Brain* **1922**;45:323–356